Research Groupin Geophysics
UNIVERSIDAD NACIONAL DE COLOMBIA

EARTH SCIENCES
RESEARCH JOURNAL

Earth Sci. Res. S J. Vol. 14, No. 2 (December, 2010): 135-144

Contribution of topographic and penetrometric measurements to a site characterization, case of the Kekem Landslide, National Road N°5 (Western Cameroon)

Jean Jacques Nguimbous-Kouoh[1, 2] and Eliezer Manguelle-Dicoum[1, 2]

[1]Department of Physics, Faculty of Science, University of Yaoundé I, P.O. Box 812 Yaoundé-Cameroon
[2] Geotech-Consulting Cameroon, Office of Geophysical Studies and Services, P.O. Box 6052 Yaoundé-Cameroon
E-mail: nguimbouskouoh@yahoo.fr

ABSTRACT

A topographical survey and a dynamic cone penetrometer testing (DCPT) were conducted over the Kekem landslide area. The aim of the work was to unveil new topographic features of the site, and with the penetrometer soundings predict the depth of the potential rupture surface beneath the damaged area. The analysis of penetrometer data has led to the supposition that the fractured surface interface connecting the basement and sediments has a depth of between 2.00 m and 12.20 m. The topographic data was used to determine the average slope percentage over the broken area. The slope percentage gives 33.66% from a point taken over the tearing niche and a point along the road. 2D contours map drawn with the Surfer software, over an area of 35 hectares has enabled the observation of a step gradient oriented NNE-SSW. Considering the steepness of the slope and the thickness of the sediments, the site remains dangerous for the populations especially during the rainy season.

Keywords: Landslide, national road N°5, kekem, topographic, penetrometer test

RESUMEN

Se hicieron un levantamiento topográfico y un ensayo con penetrómetro dinámico de cono (DCPT) sobre el área de deslizamiento Kekem. El propósito del trabajo es conocer nuevos rasgos topográficas del sitio, y con el penetrómetro predecir la profundidad a la que está la potencial superficie de ruptura debajo del área afectada. El análisis de los datos provistos por el penetrómetro ha permitido predecir que la interfaz de superficie fracturada entre el basamento y los sedimentos está a una profundidad entre 2,00 y 12,20 m. Los datos topográficos permitieron determinar la pendiente media de la zona fracturada. Medida entre un punto en la zona de desgarre y un punto a lo largo de la vía, la pendiente porcentual es de 33,66%. Líneas de contorno 2D dibujadas en el mapa con el programa Surfer, sobre una superficie de 35 hectáreas ha permitido observar un empinado gradiente orientado en dirección NNE-SSW. Tomando en cuenta la empinada pendiente y el espesor de los sedimentos, el sitio sigue siendo peligroso para la población, especialmente durante la estación lluviosa.

Palabras clave: deslizamiento de tierra, carretera nacional No. 5, Kekem, topográficos, prueba de penetrómetro

Record

Manuscript received: 20 -05- 2010
Accepted for publication: 30-11-2010

Introduction

Landslides triggered by the geology, faults or rainfalls are mostly generated in mountainous landscapes. Some of these landslides occur suddenly and flow for miles at high speeds. They may pose serious threats to life and property (Larsen et al., 2000; Agliardi et al., 2001). Landslides often take place when a swaying occurs at the fracture interface between superficial sediments and stronger bedrock. This generally results to a complete change of scenery for years or millennia (Beven, 1981; Iverson, 2000). To study the Kekem landslide zone the common subsurface geophysical methods for determining the depth of the basement top were not used because of the unfavorable environment for electrical and electrostatic methods. The slope is very rugged and electrical low tension cable disturbances nearby. We present here, the new topographic features and the results obtained using a dynamic cone penetrometer test which provides a lively alternative to conventional non destructive reconnaissance methods. This process borrowed from geotechnical studies is often used in geophysics to determine the depth of bedrock, when near the surface (Iverson and Major, 1987; Le Noble and Martinaud, 2003; Marmeta *et al.,* 2006). To illustrate how the two techniques can be combined on the field, a case study was conducted over the Kekem landslide site.

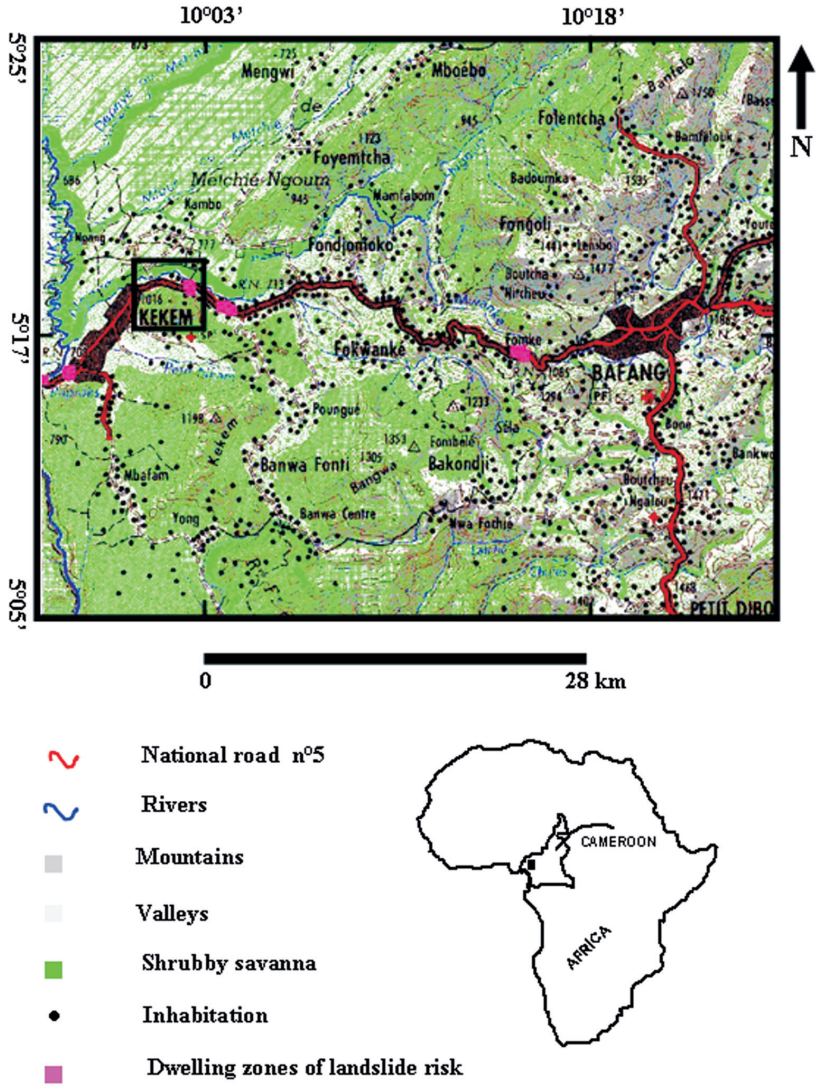

Figure 1: Location map of the study area (from Nguimbous et al., 2008)

Geographical and geological setting

The study area is located in the western region of Cameroon, between latitudes 5°05' and 5°25' North and longitudes 9°55' and 10°26' East (Figure 1). The local climate is tropical with prolonged rainy seasons from April to November. The region is heavily populated because of its economic and agricultural potentials. Geologically, the region is located in the Central African orogenic belt characterized by gneiss, which is of Proterozoic age. The local structural orientation is NNE-SSW. The outcrops in the region are in the form of isolated slabs or rocks (Kwekam, 1993; Talla, 1995; Nguiessi *et al.,* 1997).

The study area (Figure 1) belongs to the mountainous range that borders the Mbos plain. Most of the hillsides of the main mountain terrain reached their equilibrium profile since the Tertiary and Quaternary age (Belnoun *et al.,* 2008). However, their dismantling by erosion, agriculture and road works remain locally very active.

The materials able to slip are varied. They belong either to the bedrock or to the superficial formations which recover it (Talla, 1995; Nguiessi *et al.,* 1997; Nguimbous *et al.,* 2008). The rocks of the bedrock in the sector are granite-gneissic and largely metamorphosed. The shallow formations are inconsistent and are more susceptible to the rupture in the presence of groundwater, notably horizons rich in clayey minerals. The shallow formations were implemented at the rhythm of geological processes (erosion, weathering, and volcanism) of Cretaceous and Tertiary bedrock and cover the different sides with a thick deposit more or less stable.

Equipment and methodology

To cover the entire study area, we used a laser tachometer (TC 805 L) to measure the various parameters (vertical angles, horizontal and vertical drop, etc.) This equipment is made up of a long range laser (greater than 500 m) to compute inaccessible points with an accuracy of ± 3 mm (variable depending on the support quality). The site was set with a base station and secondary stations materialized by the pillars along the road and within the resident lands. The secondary stations were often used as references. They were uplifted at the beginning and at the end of the trial and led to the lift orientation and precision of successive surveys. The points were not selected according to a regular grid but according to the relief irregularities along the perpendicular and parallel lines of the hillside. A total of 397 study points were obtained including 35 penetrometer sounding points. To measure the thickness and depth of

different underground layers in several points on the site, the Dynamic Cone Penetrometer (DL010) was used. The trial test consisted to sink into the soil the stem with a cone containing a free fall mass. The stem that has at its end a cone of 20 mm in diameter sinks by dropping a hammer on its anvil. The drop height (575 mm) and the masses of the hammer (4.6 and 8 kg) are normalized according to ASTM D6951-03.

We also used a GPS for the measurement of geographical coordinates, a compass for orientation and positioning, walkie-talkies for communication and a digital camera to save and catalog the event.

Presentation of the landslide and disaster area

In October 20, 2007, after three days of intense rainfall, a landslide occurred at the entrance to the town of Kekem along National Road No5 (Figure 2). The mixture constituting multiple tons of massive materials literally slipped; destroying road, houses, plantations and killing two people.

The data obtained by direct measurements on the site were used to estimate the average height of the scratched mountain (1200 m), the average height of the road from the site relative to the sea level (723 m) and average distance between the hill and houses (4 m). The affected area corresponds to a displacement of soft soil and rock along a fracture surface (Figure 2). This earth flow occurred on a relatively steep slope, the front mass was found at 272 m from the tearing niche, stripping the soil to a depth of about 4 m. The overall movement is oriented N10 ° E dipping south. The deposits were displaced to less than 5 m from the Ngoum River, the main river of the region. The width of the stripped area varies between 18 and 55 m from the foundation of the tearing niche to the base of the material deposits. The volume of material moved is estimated to about 30.000 cubic meters. The soil profile observed at the dislocation surface reveals three different lithological levels namely: an upper horizon made up of litter and humus with thickness of about 5 centimeters, an intermediate horizon, black in colour and about 60 centimeters thick, and a lower brown, silty clay horizon that extends to the underlying bedrock (Nguimbous *et al.,* 2008).

Results and discussion

Analysis of the topographic maps

The description of a topographic map is generally intended to characterize the main aspects of the relief (Varnes, 1976; Quido and Vojtech, 1982). These main aspects can be observed on the contour maps or digital elevation models (Tucker and Whipple, 2002, Glenn *et al.*, 2006; Tarolli and Tarboton, 2006, Eeckhaut *et al.,* 2007). To realize the maps for this study, data were processed with the Covadis (2007) software which is an applicative of topography, cartography, and earthwork. The software was used for the topometric calculations and generation of the Cartesian coordinate points of the study area. These coordinates were then entered into the Surfer (2009) software for interpolation and production of contour maps and the digital elevation model (DEM). The longitudinal profile over the slipped area was generated using the Covadis (2007) software.

- The map in Figure 3 presents the site plan of the field measurement points. The points were densified at the collapsed area to better define and simulate the phenomenon.
- The 2D contour map (Figure 4) shows the distribution of altitudes in meters along the study area. The contour lines reveal a steep gradient oriented NNE-SSW, corresponding to a high escarpment of the slope. The shape of the contour lines also implies a convex slope, which is indeed remarkable in the field. The slope is gentle at the beginning but becomes increasingly steep as soon as one goes up.
- The longitudinal profile (Figure 5) over the damaged area provides an image of the topographic slope and a probable dip of geological formations and structures of the study area when going from top to bottom. From this profile, the quote lands distribution varies approximately between 780.72 and 715.27 m for a cumulative distance of about 200.41 m along the slope.
- Figure 6 shows the digital elevation model (DEM) of the study area reconstructed after topographic data interpolation. It clearly shows

Figure 2: Photographs of the landslide

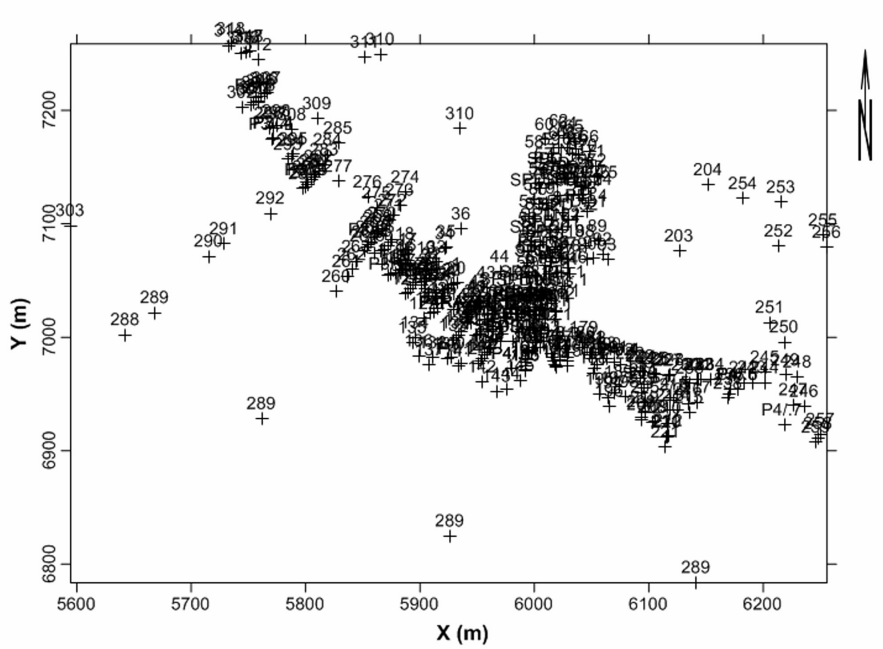

Figure 3: The site plan showing locations of the tachometer measurements points

the notch which represents the kind of landslide. Apart from the notch, the morphology of the study area appears to be homogeneous, implying a geology that remained relatively constant over time and space.

The data interpretation with the Covadis (2007) software was used to estimate the surface area covered by the study at 35 hectares, the perimeter of the area covered by the study at 1200 meters, the slipped surface area at 1.08 hectares and perimeter of 578 meters, the maximum height above the tearing niche to be 804 meters and the slope percentage over the damaged area at 35.18% for a horizontal distance of 201.04 m and a vertical distance of 70.73 m between a point taken over the tearing niche and a point along the road (Nguimbous *et al.,* 2008). Similarly, the exploitation of the 2D contour map (Figure 4) of the study area obtained with the Surfer (2009) software agreed with similar characteristics. The slope increases up with a step gradient (Figure 4). To analytically calculate the slope, we considered that there are several well-known methods for doing so (Monkhouse and Wilkinson, 1971; Denegre, 1973). The points DCPT32 (x2 y2, z2) and DCPT5 (x1, y1, z1) (Table 1) located respectively at the highest point of the tearing niche and along the road were selected. A rapid altimetric and planitmetric calculation gave (Denegre, 1973):

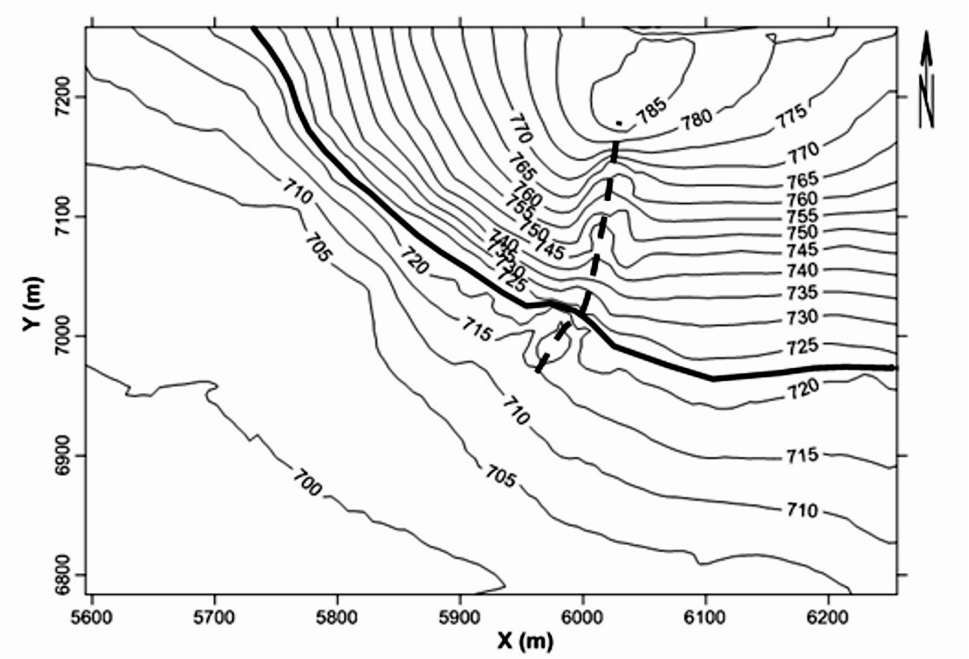

Figure 4: The 2D contour map of the study area (contour interval is 5 m) (Solid black line is National Road number 5; Dash line is longitudinal profile).

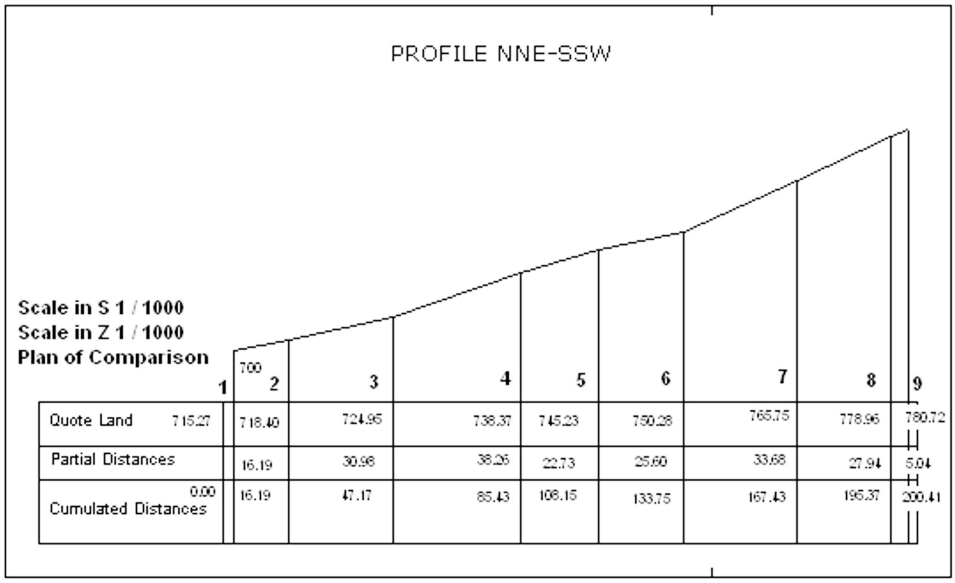

Figure 5: The longitudinal profile over the damaged area.

$$P(DCPT5;DCPT32)=\frac{|z_2-z_1|}{\sqrt{(x_2-x_1)^2+(y_2-y_1)^2}}\cdot 100=33.66\%$$

This slope is relatively similar to that obtained by Nguimbous *et al.* (2008).

In order to obtain the map (Figure 4) and the digital elevation model (Figure 6) the kriging method was used. The interpolation procedure gave for 397 introduced points, 395 active data. The semi-variogram components obtained are of linear type and the variogram slope give one. The proportion of anisotropy gives one and null angle. The (X, Y) coordinate interpolation grid gave, for values of X ranging between 5594.610 and 6255.829 m and those of Y ranging between 6783.676 and 7258.493 m, 133 lines and 96 m columns for an interpolation interval of 5 m. The grids were retained after several tests. The tightening or large interpolation interval introduces distortions on the vicinity of the points. The interpolation radius gave 407 m. The (X, Y, Z) coordinates were automatically converted into metric distance by UTM projection on the Clarke 1880 ellipsoid reference. Table 2 shows the statistical characteristics that enable the realisation of the digital elevation model (DEM) and the 2D contour map.

Analysis of table and penetrometer sounding maps

Topographic data are increasingly being combined with geotechnical data used in geophysics to determine the exact depth of basement roof (Le

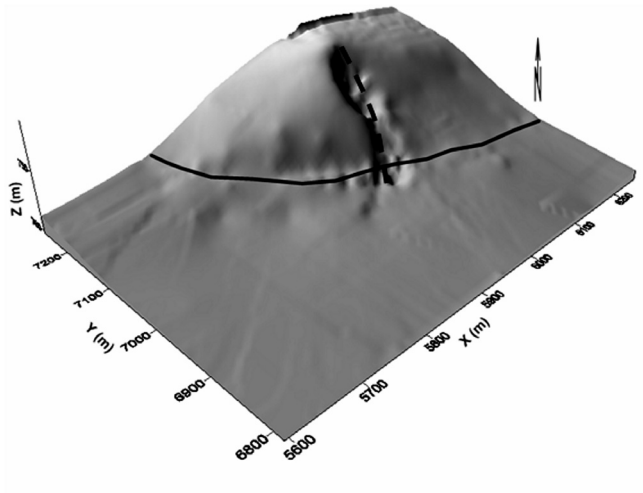

Figure 6: The 3D Digital Elevation Model (DEM) of the study area (Solid black line is National Road number 5; Dash line is longitudinal profile).

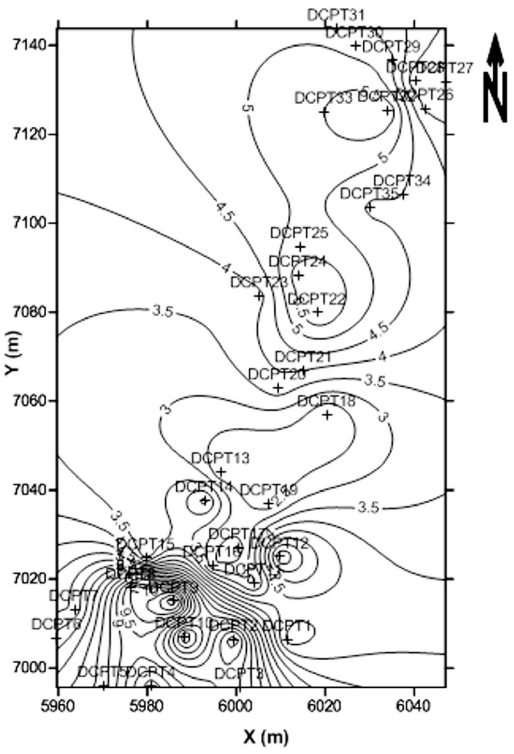

Figure 7: The map of the sediment thicknesses showing locations of the Dynamic Cone Penetrometer Testing points.

Noble and Martinaud, 2003; Falorni *et al.,* 2005; Frankel and Dolan, 2007). Two types of information were expected from penetrometer tests performed over the Kekem landslide area. That is, the height of the bedrock roof and the thickness of the sedimentary layer. The heights of the sounding were leveled with the tachometer and are correct and accurate. Thirty-five dynamic cone penetrometer testing (DCPT) were made (Nguimbous *et al.,* 2008). The results are presented in the form of maps and a table containing the depths of diverse layers beneath the slipped zone.

Table 1 highlights the Cartesian coordinates of various (DCPT) soundings. The points were identified in altimetry and planimetry. In general, the heights are irregular and ranging between 766.32 and 717.76 meters, which gives a drop of 48.56 meters between the highest point and lowest point where the measurements were made.

Table 1 equally presents the DCPT points with different depths at which the penetrometer reached. The depths are discontinuous on the entire site. The thickness of sediments was between 2.00 m and 12.20 m. The deepest sounding was obtained in DCPT9 coordinates (5985.99 m; 7015.01 m; 12.20 m).

Table 1 also shows the basement roof elevations obtained by the difference between the actual heights of the penetrometer soundings and sediment thickness acquired at different points. Overall, the elevations are asymmetrical and vary between 761.35 and 708.41 m, which give a drop of 52.94 m between the highest and lowest point of measurement.

The map of the sediment thicknesses (Figure 7) shows location of the penetrometric testing points. Its shows areas where greater sedimentary deposits thicknesses can be observe along the site. The overall sedimentary layer thickness is less important at the center of the slipped zone; it is higher at the foot of the mountain and decreases with altitude. This model-building sedimentary deposit may be correlated to the Kenyan Shurmai site (Kuehn and Adovasio, 1999).

Topographic maps of the slipped area (Figure 8a and 8b) have the same morphological features. This implies that the sediments were deposited gradually as the configuration of the basement. These maps also show that topography is irregular through out the site.

The maps (Figures 7 and 8), were obtained by the same interpolation and with the same variogram model and anisotropic coefficient like Figure 4 and 6. For 35 introduced points we obtained 35 active data and 86 m interpolation radius. The (X, Y) grid interpolation gave, for values of X ranging between 5959.690 and 6047.003 m and those of Y ranging between 6995.620 and 7143.781 m, 59 lines and 100 columns for interpolation interval of 1.50 m. The grids were tested on several occasions. For a smaller or larger interpolation interval the signal witnessed distortions.

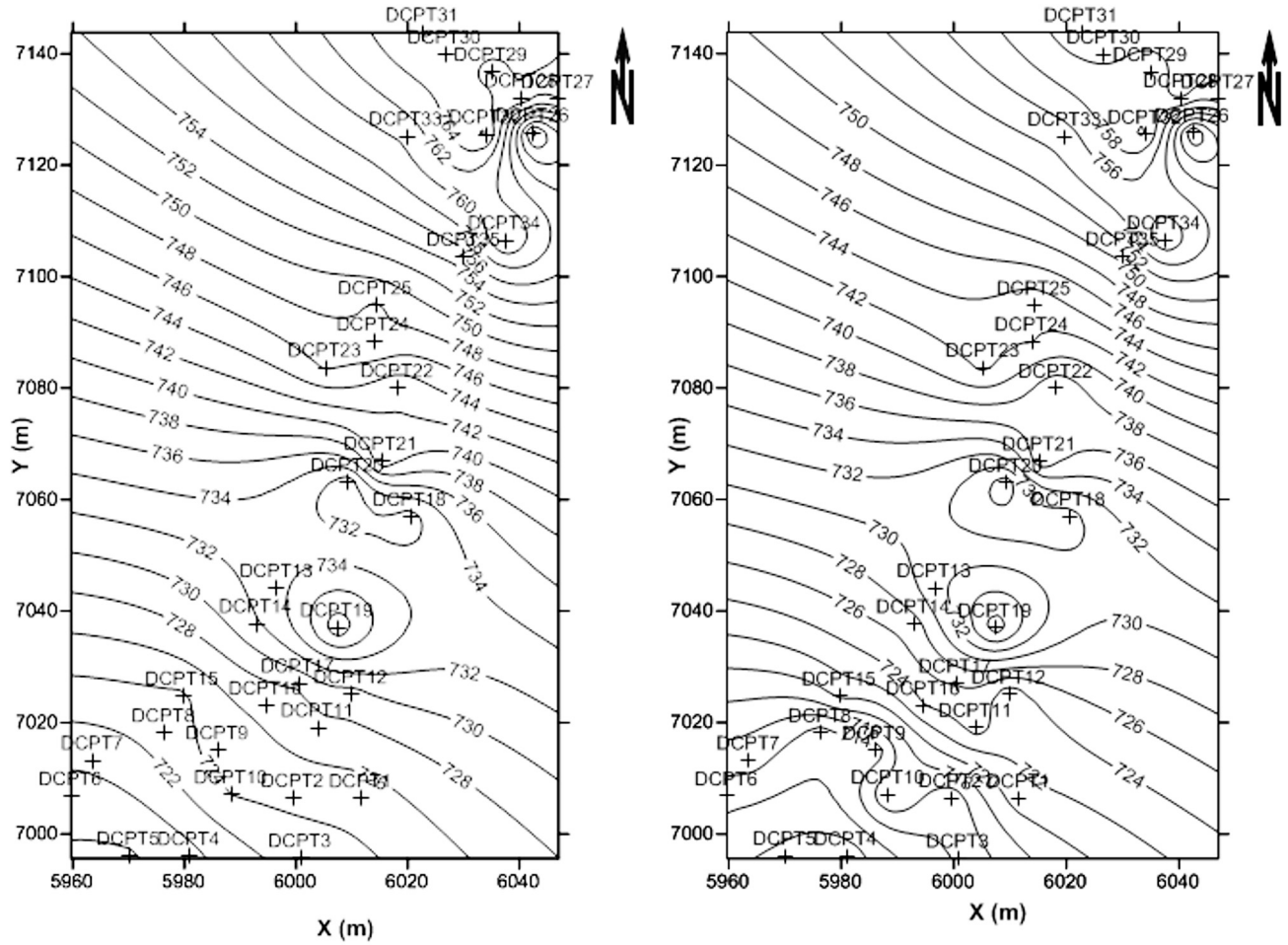

Figure 8: Topographic maps of the slipped area showing locations of the Dynamic Cone Penetrometer Testing points (Figure 8a: Topographic map of the slipped area; Figure 8b: Topographic map of the basement roof along slipped area).

Table 1: The Cartesian coordinates of the various (DCPT) sounding depths and basement roof elevations

DCPT	X (m)	Y (m)	Altitudes (m)	Depths	Basement roof elevations (m)
DCPT1	6011.62	7006.37	724.84	3.70	721.14
DCPT2	5999.50	7006.44	724.55	10.00	714.55
DCPT3	6000.81	6995.62	722.82	8.50	714.32
DCPT4	5980.90	6995.97	719.31	10.90	708.41
DCPT5	5970.05	6996.07	717.76	8.20	709.56
DCPT6	5959.69	7006.76	718.91	6.20	712.71
DCPT7	5963.63	7013.14	720.55	5.60	714.95
DCPT8	5976.36	7018.08	723.01	10.00	713.01
DCPT9	5985.99	7015.01	724.91	12.20	712.71
DCPT10	5988.42	7007.04	724.04	5.80	718.24
DCPT11	6003.97	7019.03	727.62	2.80	724.82
DCPT12	6009.88	7025.00	729.07	6.60	722.47
DCPT13	5996.60	7044.09	733.38	2.00	731.38
DCPT14	5992.91	7037.68	731.78	4.70	727.08
DCPT15	5979.69	7024.74	723.68	3.20	720.48
DCPT16	5994.64	7023.00	726.57	2.60	723.97
DCPT17	6000.41	7027.02	728.30	2.20	726.10
DCPT18	6020.47	7056.91	731.09	2.00	729.09
DCPT19	6007.41	7036.98	739.37	2.20	737.17
DCPT20	6009.31	7062.99	730.58	3.80	726.78
DCPT21	6015.27	7066.88	741.38	4.00	737.38
DCPT22	6018.21	7079.91	742.36	6.00	736.36
DCPT23	6005.26	7083.63	746.19	3.80	742.39
DCPT24	6013.97	7088.31	747.84	5.80	742.04
DCPT25	6014.29	7094.77	747.70	5.20	742.50
DCPT26	6042.44	7125.82	749.29	3.40	745.89
DCPT27	6047.00	7131.79	761.95	3.20	758.75
DCPT28	6040.41	7131.99	763.42	3.00	760.42
DCPT29	6034.98	7136.66	763.29	4.60	758.69
DCPT30	6026.69	7139.83	765.17	4.80	760.37
DCPT31	6022.71	7143.78	766.15	4.80	761.35
DCPT32	6034.01	7125.43	766.32	6.00	760.32
DCPT33	6019.78	7125.10	760.42	5.50	754.92
DCPT34	6037.48	7106.46	762.09	4.50	757.59
DCPT35	6030.10	7103.54	754.90	4.40	750.50

Table 2: The statistical characteristics of Digital Elevation Model

	X	Y	Z
Count	395	395	395
1%-tile	5715.624	6907.441	700.798
5%-tile	5761.776	6935.555	712.447
10%-tile	5807.144	6954.467	715.284
25%-tile	5903.493	6981.77	719.265
50%-tile	5994.569	7036.98	722.084
75%-tile	6040.432	7094.77	730.578
90%-tile	6118.551	7160.319	756.09
95%-tile	6177.895	7184.532	765.889
99%-tile	6246.331	7250.973	782.972
Minimum	5594.61	6783.676	700.798
Maximum	6255.829	7258.493	786.372
Mean	5976.29266329	7045.61525063	728.413065823
Median	5994.569	7036.98	722.084
Geometric Mean	5975.15577875	7045.16149688	728.216903234
Harmonic Mean	5974.01580895	7044.70915771	728.025313695
Root Mean Square	5977.42649565	7046.07041712	728.613895744
Trim Mean (10 %)	5975.84373315	7042.78160674	726.839859551
Interquartile Mean	5981.71835859	7035.64368182	722.564277778
Midrange	5925.2195	7021.0845	743.585
Winsorized Mean	5974.95846329	7044.31123544	727.579491139
TriMean	5983.26575	7037.625	723.50275
Variance	13587.9134253	6430.34244128	293.357287097
Standard Deviation	116.567205617	80.1894160179	17.1276760565
Interquartile Range	136.939	113	11.313
Range	661.219	474.817	85.574
Mean Difference	130.194017092	90.0945580672	16.6856108205
Median Abs. Deviation	65.346	55.572	3.46
Average Abs. Deviation	89.6957797468	64.4494481013	10.4998860759
Quartile Dispersion	0.0114651590662	0.00802754085876	0.00780291383274
Relative Mean Diff	0.0217850805553	0.0127873230175	0.0229067978094
Standard Error	5.86513263477	4.03476739759	0.861786908809
Coef. of Variation	0.0195049359501	0.0113814639553	0.0235136859293
Skewness	-0.160642343012	0.432891861007	1.56173296176
Kurtosis	3.1125793314	2.93037169705	4.91813436082
Sum	2360635.602	2783018.024	287723.161
Sum Absolute	2360635.602	2783018.024	287723.161
Sum Squares	14113202866.8	19610607787.6	209696892.583
Mean Square	35729627.511	49647108.323	530878.209072

The maximum depth of the basement/rupture surface varied between 2.00 and 12.20 m. These values are compatible with the supposed depths of the sediment-basement surface reached in the other risky sites (Figure 1); particularly in Marche Moume, Petit Nkam and Famke respectively located about 2, 5 and 28 km from the study area (Nguimbous *et al.,* 2008).

The study of Kekem landslide using two techniques led to the actual site characterization. This approach is comparable to conventional approaches in geophysics (Brunsden and Prior, 1984; Crozier, 1986).

Conclusion

This study, combined with the observations carried out on the field conveys evidence of the terrains fragility, the slopes steepness and the great thickness of the sediments. The risk of catastrophe for the road and the populations remains imminent; given their proximity to the site. On the other hand, the combined use of the tachometer and the dynamic cone penetrometer proved a simple and effective employment vis-a-vis of the particular problem of the site. The fluid blending of the two techniques and the data appreciably increases the productivity of the geophysicist in achievement of various tasks of precision measurement of the basement in areas where it is nearer to the surface. This approach should be validated in other sites where the relief is not very broken and the basement nearer to the surface. The method authorizes a total flexibility on the field and a successful data-gathering. The productivity of a great number of geophysics applications is thus largely improved.

References

ASTM D6951-03. (2009). Standard test method for use of the Dynamic Cone Penetrometer in shallow pavement.

Agliardi, F., Crosta, G. and Zanchi, A. (2001). Structural constraints on deep-seated slope deformation kinematics. Engineering Geology, 59: 83-102.

Belnoun, N.R.N., Tchouankoué J.P., Koller F. and Thöni M. (2008). Petrology, mineralogy, and geochemistry of Kekem mafic complex, western Cameroon. Geophysical Research, 10: 1607-7962.

Beven, K. (1981). Kinematic subsurface stormflow. Water Resources Research, 17: 1419-1424.

Brunsden, D. and Prior, D.B. (1984). Slope Instability. Wiley, Chichester 12: 102-110.

Covadis, Version 7.0. (2007). Topography, cartography, and earthwork software developed by Autodesk, dedicated to the Geometricians, Companies and Engineers.

Crozier, M.J. (1986). Landslides: Causes, Consequences, and Environment. Croom Helm, London, 59pp.

Denegre, J. (1973). Développements récents de l'automatisation appliquée aux cartes topographiques à moyenne échelle. International Yearbook of Cartography, 13: 81-89.

Eeckhaut, V.D. M., Poesen, J., Verstraeten, G., Vanacker, V., Nyssen, J., Moeyersons, J. and van Beek, L.P.H. (2007). Use of LIDAR-derived images for mapping old landslides under forest. Earth Surface Processes and Landforms, 32: 754-769.

Falorni, G., Teles, V., Vivoni, E.R., Bras, R.L. and Amaratunga, K.S. (2005). Analysis and characterization of the vertical accuracy of digital elevation models from the Shuttle Radar Topography Mission. Journal of Geophysical Research-Earth Surface, 110: 230-239.

Frankel, K.L. and Dolan, J.F. (2007). Characterizing arid region alluvial fan surface roughness with airborne laser swath mapping digital topographic data. Journal of Geophysical Research, 112: 124-135.

Glenn, N.F., Streutker, D.R., Chadwick, D.J., Tahckray, G.D. and Dorsch, S.J. (2006). Analysis of LIDAR-derived topography information for characterizing and differentiating landslide morphology and activity. Geomorphology, 73: 131-148.

Iverson, R. M., and J. J. Major. (1987). Rainfall, groundwater flow, and seasonal motion at Minor Creek landslide, northwestern California: Physical interpretation of empirical relations, Geol. Soc. Am. Bull., 99, 579–594.

Iverson R.M. (2000). Landslide triggering by rain infiltration. Water Resources Research, 36: 1897-1910.

Kuehn and Adovasio, (1999). Stratigraphy and noncultural site formation at Shurmai rockshelter (GnJm1) in the Mukogodo Hills in the north-Central Kenya. Geoarchaeology, 14: 63-85.

Kwekam M. (1993). Le massif plutonique calco-alcalin de Fomopéa (Ouest-Cameroun) : Cadre Structural, Pétrologie, Géochimie, Interprétation géodynamique. Thèse de Doctorat troisième cycle, Université de Yaoundé I, 154pp.

Larsen, M. C., Conde, V.M. T. and Clark, R. A. (2000). Landslide hazards associated with flash-floods, with examples from the December, 1999 disaster in Venezuela, in coping with Flash Floods, edited by E. Gruntfest and J. Handmer, NATO ASI Ser, 236pp.

Le Noble A. and Martinaud M. (2003). Apport du pénétromètre à la connaissance d'un site préhistorique. Cas de l'abri Diepklof, province du Cap, Afrique du Sud. Revue d'archéométrie, 27pp.

Marmeta., Faycal, R., Yu Jun, C.C., Tabbagha, A.B. and Charlerya, Y. (2006). Correlations between geotechnical and electrical data: A case study at Garchy in France. Journal of Applied Geophysics, 60: 165-178.

Monkhouse, F.J. and Wilkinson, H.R. (1971). Maps and Diagrams; their compilation and construction, Gradient and Slope. Londres, Methuen & Co. Ltd, 3: 129-165.

Nguiessi, C., Nzenti, J.P., Nkonguin, N.E., Tempier, P. and Tchoua, F. (1997). Les granitoïdes calco-alcalins, syn-cisaillement de Bandja dans la chaîne panafricaine nord équatoriale au Cameroun. C. R. Acad. Sci. Paris, Sciences de la Terre et des planètes, 325 : 95-101.

Nguimbous, K. J.J. Epada J. and Manguelle, D.E. (2008). Rapport de l'étude topographique sur le glissement de terrain de la route nationale n° 5 à Kekem. Pour le Labogenie, 100pp.

Quido, Z. and Vojtech, M. (1982). Landslides and their control. Elsevier Scientific Publishing Company Amsterdam. 56pp.

Surfer(R) Version 9.0. (2009). Contouring and 3D Surface Mapping for Scientist and Engineers. Golden Software, Inc., Colorado, U.S.A.

Talla, V. (1995). Le massif granitique panafricain de Batié (Ouest-Cameroun) : Pétrologie, Pétrostructurale, Géochimie. Thèse de Doctorat troisième cycle, Université de Yaoundé I.128pp.

Tarolli, P. and Tarboton, D.G. (2006). A new method for determination of most likely landslide initiation points and the evaluation of digital terrain model scale in terrain stability mapping. Hydrology and Earth System Sciences, 10: 663-677.

Tucker, G. E. and Whipple, K.X. (2002). Topographic outcomes predicted by stream erosion models: Sensitivity analysis and intermodel comparison. J. Geophys. Res, 107: 2170-2179.

Varnes, D. J. (1976). Slope movement types and processes. National Academy of Sciences, Spec, Report 36pp.

Acknowledgments

The authors thank the reviewers for their comments and suggestions which enabled to improve the initial version of the manuscript.